

# Statistical Transduction ... an Introduction to Holometrics

George Fox Lang, Fox Technology Corporation, Glen Rock, New Jersey  
Clifford T. Gunsallus, Kaman Aerospace Corporation, Bloomfield, Connecticut

Measuring the dynamic strains, motions and forces at play within the rotating elements of a machine is always a difficult task. Slip-rings and/or telemetry equipment have been successfully employed for such studies in the laboratory, but these are expensive and temperamental solutions ill-suited to continuous monitoring applications. Recent experience with a new technology termed "Holometrics" is examined here; unique signal processing of redundant fixed-system sensors is shown to be a valid means of measuring rotating-system parameters.

There are many motivations driving the desire to measure strains and motions within the rotor system of a helicopter. Paramount among these are realistic measurement of life-consumption of blades and other rotating components and direct detection of events leading to excitation of the fuselage.

The reliability/maintainability of slip-ring and rotating-telemetry based transducer installations has failed to meet the stringent requirements placed upon fully certificated commercial and military aircraft. While these devices have proved useful in development flights with experimental aircraft, they have not become integral airframe components.

Critical and expensive rotor system components must be changed out of an aircraft based solely upon operating hours. Most of these components are exchanged long before their structural life has been fully utilized as the timing for such action is conservatively based upon a "worst case" assumption of flight operation. If all helicopters were actively engaged in battle, these "must change" intervals would still be conservative, but would be realistic. Fortunately, most of these vehicles live a far more sedate life but this implies excessive operating costs. The ability to directly monitor blade, hub and control system loads on a continuous basis has long been sought. Such measurements will permit real-time evaluation of the remaining service life based upon the loading *actually experienced* by the hardware.

Additionally, such measurements are required inputs for proposed rotor control optimization systems aimed at minimizing loads experienced by both the rotor and the airframe. Such systems invariably include "higher harmonic" control inputs aimed at reducing loads by countermanding undesired vibration caused by aerodynamic reaction to normal collective and cyclic pitch commands.

Research at Kaman Aerospace Corporation is on-going in all aspects of helicopter design and improvement. A recent benefit of these programs is the development of the "Holometric Synthesizer," a device that monitors rotor parameters without the need for a slip-ring. This dedicated purpose Fourier-based computer was designed and constructed by Fox Technology acting under contract to Kaman Aerospace which has applied for patents protecting the device and its underlying methods and principles.

The instrument's technical basis is part of a larger mathematical philosophy termed "Holometrics" from the Greek *holokos*, meaning whole and *metron*, to measure. In essence, Holometrics capitalizes upon the simple fact that any piece of information in a physical process is expressed with great redundancy throughout that process. This allows any variable of the process to be "viewed" by observing other variables of the process and inferring the required information. A clear picture is obtained when an appropriate vantage point from which to

observe the *unique* content of that information is mathematically selected.

In this article we will discuss statistically transducing blade bending moments from an SH-2 class helicopter and will compare the results to those of direct transduction through slip-rings. The test aircraft is shown in Figure 1 which details the arrangement of sensors employed.

The blade-mounted strain gauges and slip-ring shown are used solely as a calibration reference. The sensors actually employed in the statistical transduction are the strain gauges fitted to the eight transmission support tubes that attach the rotor system to the fuselage. Additionally, a magnetic pick-up within the transmission is used to provide a once-per-turn rotor tachometer signal.

The support tube strains and the tachometer signal were processed in real time by the "HALMARS Holometric Synthesizer" shown in Figure 2. This device produced an analog blade bending moment output signal from the fixed system inputs. As subsequently demonstrated, this signal faithfully reproduced the directly transduced measurement throughout the flight envelope.

## A Brief Review of Rotor Characteristics

The dynamics of a helicopter rotor are quite involved. While we will not digress to a development of rotor vibration equations, several salient properties of operating rotors need to be understood:

1. The forces and moments developed by the rotating blades are dominated by periodic components at the rotor frequency and its harmonics. For a variety of reasons, rotors operate within a narrow speed range.
2. Rotors are symmetric; the blades are very closely matched and trimmed with regard to aerodynamic shape, stiffness and inertia distribution and are uniformly spaced.
3. The blades are "loosely attached" to the rotor hub using multiple hinges and/or elastomeric bearings. This is done to minimize the "flatwise" and "edgewise" moments experienced by the blades and to facilitate cyclic and collective pitch positioning, effecting directional control.
4. Blade reactions sum at the rotor hub to form the loads transmitted to the fuselage. The symmetric disposition of the blades and periodic nature of their excitation cause many components of these summations to be zero-valued. Hence, the rotor (as a whole) acts as an order-sensitive "notch filter." Only a limited set of excitation harmonics ever reach the fixed system.
5. Forces and moments transmitted to the fuselage from the hub are not (necessarily) at the same frequency in both the fixed and rotating systems. A hub force or moment described by a sinusoidally varying vector perpendicular to the plane of the rotor results in a similar vector in the fixed system at the same frequency. An "in plane" hub vector behaves differently, resulting in fixed system reactions at a frequency equal to the rotating system frequency **plus or minus the rotor frequency**.

Consider the  $n$ th blade of an  $N$ -bladed rotor as in Figure 3. At the point of attachment with the rotor hub, the hub reactions may be decomposed into three mutually perpendicular directions as shown. These reactions consist of the radial  $R_n$ , flatwise  $F_n$  and edgewise  $E_n$  shear forces and moments about these

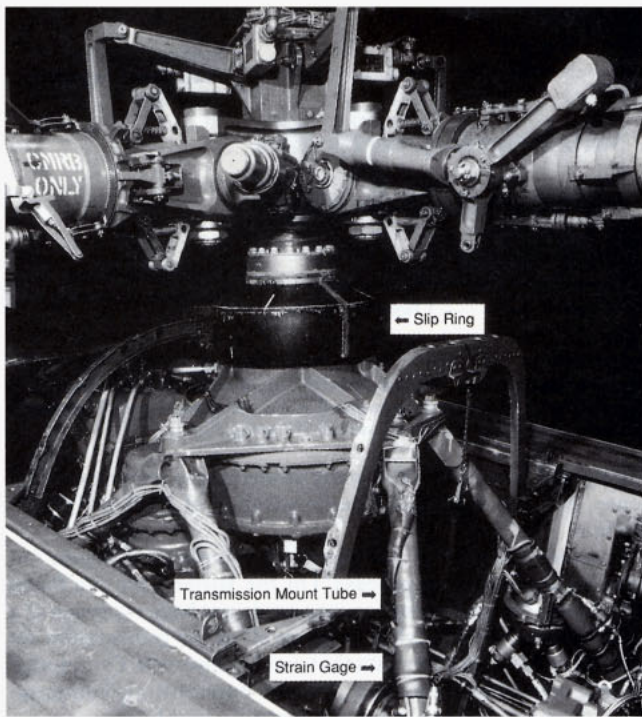


Figure 1. SH-2 rotor head, transmission and support tubes with strain gauge locations marked. Note slip-ring assembly used in calibration flight.

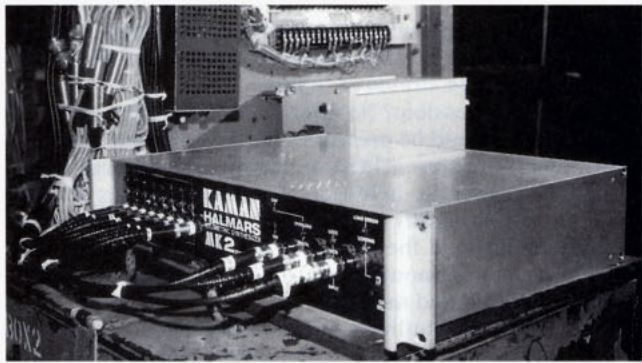


Figure 2. Mark 2 Synthesizer installed for preliminary test flights.

same axes. Each blade is separated from its neighbor by an angle of  $2\pi/N$  radians and the rotor turns about a vertical  $Z$  axis at a rate of  $\Omega$  radians per second.

The six reactions will each be periodic functions of blade position. For simplicity, we will merely deal with the three *vector directions* as the subsequently discussed transforming effects on shears and moments are identical. As these loads are periodic, they may be represented by a Fourier Series of  $\Omega$  and its integer harmonics. Hence the reactions at the  $k$ th multiple of rotor speed may be written:

$$\begin{Bmatrix} R_n \\ F_n \\ E_n \end{Bmatrix} = \begin{Bmatrix} R_c & R_s \\ F_c & F_s \\ E_c & E_s \end{Bmatrix} \begin{Bmatrix} \cos k\Omega t \\ \sin k\Omega t \end{Bmatrix} \quad (1)$$

The total reaction *on the rotating hub* due to all  $N$  blades may be formed by summation. We will form these sums to a rotating axis set  $x', y', z'$  identical to the  $R, E$  and  $F$  directions of the  $N$ th blade, respectively. This results in:

$$\begin{Bmatrix} x' \\ y' \\ z' \end{Bmatrix} = \begin{Bmatrix} R_c & R_s & -E_s & E_c & 0 & 0 \\ E_c & E_s & R_s & -R_c & 0 & 0 \\ 0 & 0 & 0 & 0 & F_c & F_s \end{Bmatrix} \begin{Bmatrix} \alpha_{kN} \cos k\Omega t \\ \alpha_{kN} \sin k\Omega t \\ \beta_{kN} \cos k\Omega t \\ \beta_{kN} \sin k\Omega t \\ \gamma_{kN} \cos k\Omega t \\ \gamma_{kN} \sin k\Omega t \end{Bmatrix} \quad (2)$$

The greek-symbol coefficients are a function of the rotor

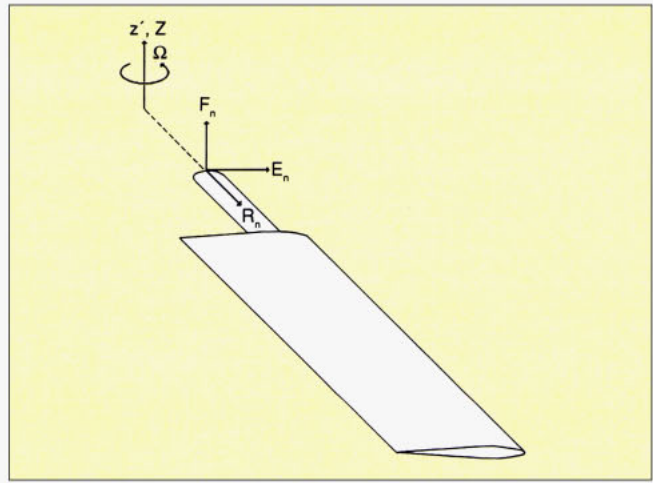


Figure 3. Radial, flatwise and edgewise forces at each blade attachment.

harmonic  $k$  and the number of blades  $N$ . These are defined in the following tables. Note that the two-bladed configuration represents a special case; this is described by Table 2. All other other (practical) configurations are described by Table 1.

From the preceding we note that only a limited number of harmonics can lead to non-zero sums. Only the vertical ( $z'$ ) direction passes a steady or 'dc' term. This direction can also exhibit harmonic content at *any* integer multiple  $m$  of the blade passage frequency  $N\Omega$ .

The "in-plane" ( $x'$  and  $y'$ ) directions behave differently. Here the hub can exhibit (rotating) reactions at the rotor frequency  $\Omega$  and at multiples of the the blade passage frequency *plus or minus*  $\Omega$ .

Hence, the rotating hub only exhibits net forces and moments at frequencies of  $(m-1)N$ ,  $mN$ , and  $(m+1)N$  times the rotor speed  $\Omega$ . While the hub and blades experience stress and strain at virtually all harmonics of  $\Omega$ , only these limited frequencies are available to plague the airframe.

Now consider how these excitations transform to the  $X, Y$  and  $Z$  fixed system directions. We will presume  $X$  to be the forward or flight direction,  $Y$  to be port (pilot's left) and  $Z$  to be vertical.

Clearly the  $Z$  and  $z$  directions are synonymous and we make no new discoveries in this direction. However,  $x'$  and  $y'$  rotate about  $Z$  with respect to  $X$  and  $Y$  at frequency  $\Omega$ . This results in an amplitude modulation or heterodyning process because the in-plane reactions are multiplied by  $\sin(\Omega t)$  and  $\cos(\Omega t)$ . Multiplication of sinusoids at  $\Omega t$  and  $k\Omega t$  gives rise to terms at  $(k-1)\Omega t$  and  $(k+1)\Omega t$  and we find:

$$\begin{Bmatrix} x \\ y \\ z \end{Bmatrix} = \begin{Bmatrix} 0 & 0 & (R_c - E_s) & (E_c + R_s) & (R_c + E_s) & (E_c - R_s) \\ 0 & 0 & (E_c + R_s) & (E_s - R_c) & (E_c - R_s) & (R_c + E_s) \\ F_c & F_s & 0 & 0 & 0 & 0 \end{Bmatrix} \begin{Bmatrix} \gamma_{kN} \cos k\Omega t \\ \gamma_{kN} \sin k\Omega t \\ \delta_{kN} \cos (k-1)\Omega t \\ \delta_{kN} \sin (k-1)\Omega t \\ \epsilon_{kN} \cos (k+1)\Omega t \\ \epsilon_{kN} \sin (k+1)\Omega t \end{Bmatrix} \quad (3)$$

Table 1. Coefficients by harmonic order for rotors with  $N = 3$  or more blades.

	$\alpha_{kN}$	$\beta_{kN}$	$\gamma_{kN}$	$\delta_{kN}$	$\epsilon_{kN}$
$k = 0$ .....	0	0	$N$	0	0
$k = 1$ .....	$N/2$	$N/2$	0	$N/2$	0
$k = mN - 1$ .....	$N/2$	$-N/2$	0	0	$N/2$
$k = mN$ .....	0	0	$N$	0	0
$k = mN + 1$ .....	$N/2$	$N/2$	0	$N/2$	0

Table 2. Coefficients by harmonic order for rotors with  $N = 2$  blades.

	$\alpha_{kN}$	$\beta_{kN}$	$\gamma_{kN}$	$\delta_{kN}$	$\epsilon_{kN}$
$k = 0$ .....	0	0	2	0	0
$k = \text{even}$ .....	0	0	2	0	0
$k = \text{odd}$ .....	2	0	0	2	2

At first glance, the in-plane results are reminiscent of a “balanced” or “suppressed carrier” amplitude modulation, where in conjugate spectral term pairs appear symmetrically disposed around the carrier frequency. This occurs with a two-bladed machine but is not a general result.

Inspection of Table 1 discloses that the  $\delta$  and  $\epsilon$  terms are never simultaneously non-zero for a rotor of 3 or more blades. That is, any harmonic that can exert a reaction upon the fuselage is heterodyned to a single frequency, not a pair of frequencies. Hence the modulation mechanism is of “single-sideband” form.

With regard to the four-bladed rotor of the SH-2 helicopter, only the harmonic terms listed in Table 3 can be detected in the fixed system, regardless of the frequencies detectable upon a single blade.

Caveats apply to the preceding. First, we have developed our frequency list based upon the assumption of a perfectly symmetric system. This is not unwarranted; rotor systems are carefully fabricated, inspected and tested to preclude “maverick” blades. Rotors are finely balanced and tracked routinely. Lag damper rates are closely matched and structural isotropy is verified by test. Nonetheless, dissymmetries *can* produce terms at frequencies not included in Table 3. These are invariably of small amplitude or the machine is subjected to maintenance to make them so.

Second, the main rotor is not the only source excitation! At minimum, the yaw-controlling tail rotor, its drive shaft, the transmission and the engines must be considered reasonable candidates for the production of fuselage terms at harmonics of the rotor speed. Further, the rotor down-wash is harmonically rich and never manages to completely avoid the fuselage in its desperate search for equilibrium.

Third, the fixed-system *directions* of Table 3 refer to a triad at the rotor’s center, far above the fuselage. Forces can be produced along these axes and moments are produced *around* them. These directions should not be interpreted as the only directions of possible fuselage response.

### Of Sorcery and Horse Sneakers

The salient point of the foregoing was to demonstrate that the fuselage loads *due to blade behavior* do not contain all possible harmonics experienced by the blades. Further, the fuselage responses do not contain terms **directly** representative of all possible blade harmonics. “Directly” is a key word, here; this “sparse” information is actually sufficient to accurately transduce the blade’s full harmonic behavior. In fact, we have *more* information than is required.

If the loading relationships between the blades and the fuselage were simple linear “mixings,” the process would be intuitively obvious. Our strain gauge laboratory at GM Proving Grounds used an ancient horseshoe to demonstrate the solution of such problems. Old Dobbins’s Reebok™ was fitted with a myriad of haphazardly oriented strain gauges. One of its heel calks was welded to a base plate and a loading block was welded to the other. All angles of assembly were capriciously selected and never recorded. For lasting beauty the shoe was finished in a delicate patina of rust.

As crude as this device appeared, it was actually a very precise triaxial load and torque gauge. Careful calibration tests allowed formulation of a matrix which resolved the desired six

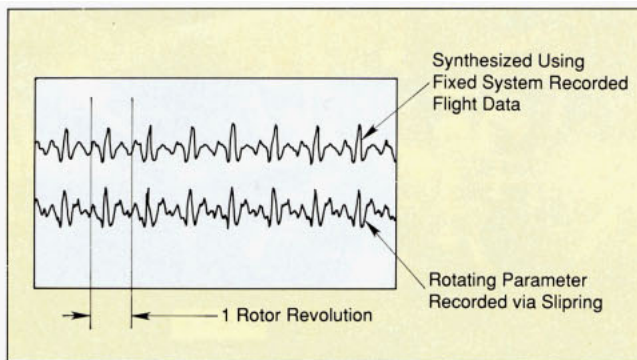


Figure 4. Comparison of Holometrically Synthesized and slip-ring transduced flatwise blade bending moment over approximately eight rotor revolutions in straight and level, nonaccelerating flight.

orthogonal loads from the many strain gauge responses. In a sense, this was a simplistic demonstration of statistical transduction.

However, the case at hand is more complicated; we do not have a simple mixing process. On the surface, we are faced with a major impediment because we do not have evidence of a “closed form” relationship between all of the information we want to resolve with the data that can be observed. Our choice of implementing frequency domain curve-fitting computations does not appear to circumvent this problem.

In our test aircraft, fuselage strains at dc and frequencies 1,4,8, . . . 4m per revolution were anticipated (and observed). These represent incomplete descriptions of blade activities at dc and 1,3,4,5,7,8,9, . . . (4m + 1) per revolution. Nonetheless, we successfully transduced blade bending moments to a bandwidth of 6Ω, in this instance using *only* the dc and 4Ω components of the 8 tube strains as inputs.

How was this possible? No information caused by 2Ω or 6Ω blade activity should be present in the fixed system, yet these components were present in blade bending and properly transduced. The answer lies in the fact that the harmonics of blade strain are *not* physically independent entities. While we may not fully understand the nature of the physical dependence between various harmonic terms, it does exist and can be statistically detected and modeled.

Every reader is intuitively aware of this phenomenon. We have no difficulty in recognizing the unique “voices” that make up the composite sound of an orchestra. Each instrument exhibits a signature relationship among the various harmonics it generates. The human ear and brain have no difficulty in utilizing this information to differentiate between a cornet and a trombone.

We are not discussing evil witchcraft here, we are merely observing and respecting physical realities. The motions and strain propagation paths of any structure are prescribed by its modal properties in consort with the specifics of its excitation. Forcing motion in any prescribed manner implies imparting energy to all of the modes and this, in turn, prescribes certain physical constraints upon the required excitation spectrum.

The underlying relationships between harmonic variables can be seen if we “strip away” those redundancies that mask our ability to see them. Holometrics filters all of the available observations and selects a minimum dimension set of statistically independent harmonic variables. From these, a minimized-error linear expression for the Fourier coefficients of the desired measurand is formed.

As with “Dobbins Reebok,” the measurement system must be calibrated, in this instance through a one-time test flight involving blade sensors and slip-rings. As with the horseshoe, the result of this effort is also a matrix, the elements of which are termed the *Holometric Coefficients*. These coefficients prescribe the ratio the Fourier coefficients of the desired rotor variable to specific Fourier coefficients measured from the available fixed-system signals.

The matrix of Holometric Coefficients is, in general, non-

Table 3. Fixed system frequencies for SH-2 helicopter.

Detected in Fixed System		Blade Source	
Frequency	Direction	Frequency	Direction
0	Z	0	F
0	X, Y	1	R, E
4Ω	X, Y	3Ω	R, E
4Ω	Z	4Ω	F
4Ω	X, Y	5Ω	R, E
4mΩ	X, Y	(4m - 1)Ω	R, E
4mΩ	Z	4mΩ	F
4mΩ	X, Y	(4m + 1)Ω	R, E

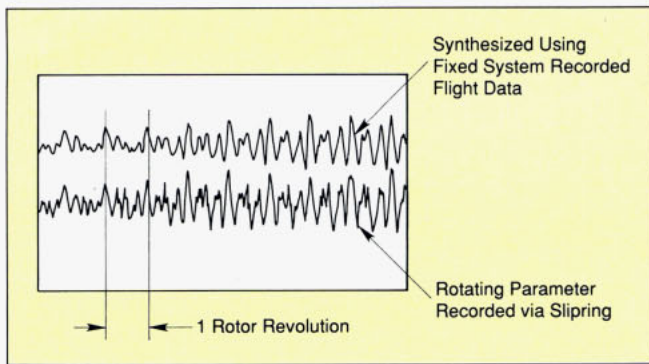


Figure 5. Comparison of Holometrically Synthesized and directly transduced transient flatwise blade bending moment over several rotor revolutions during a 1.8 g "pull-up" maneuver.

square with more input terms than required outputs. These coefficients are global to the operational envelope of the helicopter; that is, a single matrix characterizes a variable over the spectrum of flight possibilities. Clearly, this imposes the constraint that the calibration flight be as general as possible so that the matrix encompasses all mission expectations.

### Proof of the (JELLO?) Pudding

The preceding discussion may be deemed somewhat arcane. The following figures should dispel any notion that we are dealing in heretical arts. Several blade, hub and control system parameters were monitored and correlated; all fared well. The following two examples were not selected because they were the "best match" data available; they were selected because they represented two radically disparate flight situations and reflect data that are rich in harmonic terms not directly transmitted to the fuselage. In short, they represent what might be termed "tough cases."

In Figure 4, eight rotor cycles ( $\approx 1.6$  sec) of flatwise blade bending moment are presented. Two similar traces are shown, the upper trace being holometrically synthesized from the transmission support tubes and the lower trace measured directly through a slip-ring. These traces represent a "steady-state" level flight condition at 40 knots. The helicopter is "straight and level" and not maneuvering.

This correlation is typical of forward flight at any velocity within the operational envelope. The differences between the two traces in Figure 4 are dominated by terms above the 6 $\Omega$  range synthesized. Clearly, the statistical transduction faithfully models the direct measurement.

Figure 5 represents a more stringent test of the measurement methodology. Here we compare flatwise blade bending during a transient maneuver, a 1.8g "pull-up." The pilot initiated this maneuver from straight and level flight by abruptly applying a positive collective pitch input, causing the vehicle to rise rapidly while forward velocity decayed. Note the strong similarity between the holometrically synthesized (upper) and directly transduced (lower) data traces in all characteristics. For purposes of stress evaluation, these traces are interchangeable.

### How Was This Done?

The signal to be transduced has the form . . .

$$y(t) = A_0 + \sum_{k=1}^{\infty} [A_k \cos(k\Omega t) + B_k \sin(k\Omega t)] + N(t) \quad (4)$$

. . . where  $N(t)$  represents nonperiodic "noise." This signal is approximated by a "noise-free" estimator truncated to a desired number of rotor harmonics. In the preceding examples, 6 rotor orders were included and we approximated the function of (4) by:

$$\bar{y}(t) = A_0 + \sum_{k=1}^6 [A_k \cos(k\Omega t) + B_k \sin(k\Omega t)] \quad (5)$$

The required Fourier coefficients are derived by multiplying a

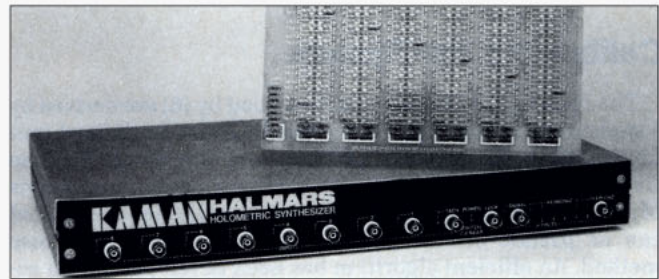


Figure 6. Mark 1 HALMARS Holometric Synthesizer and analog programming board.

vector of Fourier coefficients measured from the fixed system by a matrix of Holometric Coefficients established from a prior calibration flight. For example:

$$\begin{matrix} A_0 \\ A_1 \\ B_1 \\ A_2 \\ B_2 \\ \vdots \\ A_6 \\ B_6 \end{matrix} = \begin{matrix} C_{1,1} & C_{1,2} & \dots & C_{1,24} \\ \vdots & \ddots & \ddots & \vdots \\ \vdots & \vdots & C_{ij} & \vdots \\ \vdots & \vdots & \vdots & \vdots \\ C_{13,1} & \dots & \dots & C_{13,24} \end{matrix} \begin{matrix} a_{01} \\ a_{r1} \\ b_{r1} \\ \vdots \\ a_{08} \\ a_{r8} \\ b_{r8} \end{matrix} \quad (6)$$

$\begin{matrix} 13 \times 1 & & & 13 \times 24 & 24 \times 1 \end{matrix}$

In the example instance, 13 output coefficients (dc plus 6 sines and 6 cosines) are developed from 24 detected input coefficients. The input coefficients consist of a dc ( $a_0$ ), a cosine ( $a_r$ ) and a sine ( $b_r$ ) coefficient detected from each of 8 strain gauges. All harmonic coefficients employed were those of blade passage frequency  $r = 4$ .

The required input Fourier coefficients are derived from their formal definition with measurement averaged over one rotor revolution. Specifically:

$$a_{0j} = (\Omega/\pi) \int_0^{2\pi/\Omega} x_j(t) dt \quad (7a)$$

$$a_{rj} = (\Omega/\pi) \int_0^{2\pi/\Omega} x_j(t) \cos(r\Omega t) dt \quad (7b)$$

$$b_{rj} = (\Omega/\pi) \int_0^{2\pi/\Omega} x_j(t) \sin(r\Omega t) dt \quad (7c)$$

These computations are performed in real-time by a dedicated purpose processor, a "Holometric Synthesizer." Two versions of this machine were built during the span of this project.

In 1986 Fox Technology delivered the initial HALMARS Holometric Synthesizer prototype shown in Figure 6. This machine relied heavily upon analog processing, although it contained many digital and hybrid elements. Analog computation of the matrix multiplication of (6) was employed, with the matrix programmed by installing precision resistors on a replaceable printed circuit board as shown. The machine was restricted to ac coupled analysis and synthesis for up to 6 harmonic orders. It incorporated a unique rotor synchronization circuit termed a "period lock loop with phase assertion" (PLL/PA).

In 1988 Fox developed the Mk 2 instrument shown in Figure 7. This device is modular and expandable. It implements the matrix multiplication and synthesis in a completely digital fashion. Its real-time bandwidth is 3 kHz with future capability of 30 kHz operation for other applications. The instrument retains 32 switch selectable Holometric matrices, each of 408 coefficients. Each input channel is a dc coupled, gain-programmable differential amplifier. Each channel detects dc and the quadrature components at any programmable rotor order, 1 through 8. The output contains dc and 8 rotor orders. The Mk 2 is programmed by down-loading from an IBM<sup>®</sup> compatible PC.

Both machines employ the same hybrid method of "order normalized" Fourier coefficient detection. High temporal pre-

## Calibrating the System

The Holometric Coefficients described by (6) are derived by a statistical methodology employing the Jones Euclidian Limit Length Orthogonalization (JELLO) and the Moore-Penrose Generalized Inverse. The JELLO is a Kaman developed means of selecting data vectors to form a well-conditioned matrix that can be pseudo-inversed by the well-known Moore-Penrose method. An efficient algorithm has been developed which actually performs this selection in the process of computing the pseudo-inverse. For clarity of explanation, these matters are presented separately here.

First, equation (6) may be restated in more general form; specifically:

$$\begin{matrix} \left\{ A \right\} \\ n \times 1 \end{matrix} = \begin{matrix} \left[ C \right] \\ n \times m \end{matrix} \begin{matrix} \left\{ a \right\} \\ m \times 1 \end{matrix} \quad (8)$$

This is the synthesis equation implemented in real-time, using  $m$  measured fixed-system Fourier coefficients  $\{a\}$  to compute  $n$  desired rotating-system coefficients  $\{A\}$ . The  $[C]$  matrix contains the Holometric Coefficients and is, in general, non-square. This matrix is derived from a series of flight test measurements.

A series of  $f$  flight condition measurements is made and the data arranged in the following calibration equation:

$$\begin{matrix} \left\{ a \right\} \\ f \times m \end{matrix} \begin{matrix} \left[ C^T \right] \\ m \times n \end{matrix} = \begin{matrix} \left\{ A \right\} \\ f \times n \end{matrix} + \begin{matrix} \left\{ \epsilon \right\} \\ f \times n \end{matrix} \quad (9)$$

In (9), solution for the transpose of the unknown  $[C]$  matrix is sought from matrices involving direct measurement of the desired coefficients  $\{A\}$  and all potential monitoring coefficients  $\{a\}$ . These are arranged in matrices where each row represents a specific flight condition and each column contains a single specific Fourier coefficient. The  $\{\epsilon\}$  matrix contains the errors associated with the fit of  $[C]$  to the data of the  $\{a\}$  and  $\{A\}$  matrices. A solution is sought which minimizes these errors. Note that the dimension of the  $[C]$  matrix is independent of the number of flight conditions  $f$  employed for calibration.

If the information content of each  $\{a\}$  column is unique, the minimum error solution of (9) is given by the Moore-Penrose Generalized Inverse. That is:

$$\begin{matrix} \left[ C^T \right] \\ m \times n \end{matrix} = \begin{matrix} \left[ a^T a \right]^{-1} \\ m \times m \end{matrix} \begin{matrix} \left[ a^T \right] \\ m \times f \end{matrix} \begin{matrix} \left\{ A \right\} \\ f \times n \end{matrix} \quad (10)$$

Unfortunately, we have no guarantee of such informational independence. Each column in  $\{a\}$  merely reflects our decision to process a specific rotor-order harmonic coefficient from a specific fixed-system transducer. In general, we must presume  $\{a\}$  to be ill-conditioned for our purpose. While we may be successful in the numeric exercise of inverting  $\{a^T a\}$  and evaluating  $[C^T]$ , the solution will not be physically meaningful.

The solution to this problem is to select informationally independent  $\{a\}$  columns before implementing (10). This is accomplished by measuring more fixed-system data columns (i.e. more sensor locations and/or more Fourier terms from each sensor) than are required and then "filtering through" the available data to select a minimum number of meaningful columns.

This process is implemented by the recursive JELLO algorithm, which qualifies a "trial" column in terms of previously accepted columns. This qualification is provided by an "angle of independence"  $\alpha$  computed from the trial column vector and the matrix of previously accepted vectors. If this angle equals or exceeds an acceptance threshold, the trial vector is deemed informationally independent and is added as a column of the  $\{a\}$  matrix. Vectors exhibiting  $\alpha$  less than the threshold angle are discarded.

Clearly, any *single* column alone represents independent information. Hence, the process can be initiated (i.e.  $m = 1$ ) by selecting any single observation column as a "seed" for  $\{a\}$ . Thereafter,  $\{a\}$  is sequentially enlarged by appending a successfully tested additional column vector,  $\{v\}$ , in the fashion:

$$\begin{matrix} \left\{ a \right\} \\ f \times (m+1) \end{matrix} = \begin{matrix} \left\{ a \right\} \\ f \times m \end{matrix} \begin{matrix} \left\{ v \right\} \\ f \times 1 \end{matrix} \quad (11)$$

In (11), the right-hand side  $f \times m$  matrix  $\{a\}$  represents a set of previously tested and accepted measurement columns.  $\{v\}$  represents new information to be appended, incrementing the size of the  $\{a\}$  matrix to  $f \times (m + 1)$ . Before the left-hand matrix of (11) is formed, the associated angle of independence  $\alpha$  is determined from:

$$\alpha = \cos^{-1} \left( \frac{\begin{matrix} \left\{ v^T \right\} \\ 1 \times f \end{matrix} \begin{matrix} \left\{ a \right\} \\ f \times m \end{matrix} \begin{matrix} \left[ a^T a \right]^{-1} \\ m \times m \end{matrix} \begin{matrix} \left\{ a^T \right\} \\ m \times f \end{matrix} \begin{matrix} \left\{ v \right\} \\ f \times 1 \end{matrix} \right)^{1/2} \quad (12)$$

That is,  $\alpha$  is determined from two scalars formed by suitable vector and matrix operations performed upon the trial vector,  $\{v\}$  and the *previously* accepted  $\{a\}$  matrix. Equation (12) defines the angle of independence from the vector's length and its generalized length with respect to the informational space of  $\{a\}$ .

The threshold angle against which  $\alpha$  is tested is a function of the estimated precision of the measurements employed. From statistical considerations we can establish a relationship between the estimated fractional random error  $\pm e$  of each measurement and the minimum required threshold angle  $\alpha_t$ ; specifically:

$$\alpha_t = \cos^{-1} \left( 1 + \frac{e}{3} \right)^{-1/2} \quad (13)$$

From (13) we may evaluate typical threshold angles for increasing levels of data contamination as presented in Table 4.

Table 4. Estimated random measurement error versus minimum angle of independence.

Error	Angle	Error	Angle
±5%	1.65°	±20%	6.59°
±10%	3.30°	±25%	8.21°
±15%	4.95°	±30%	9.83°

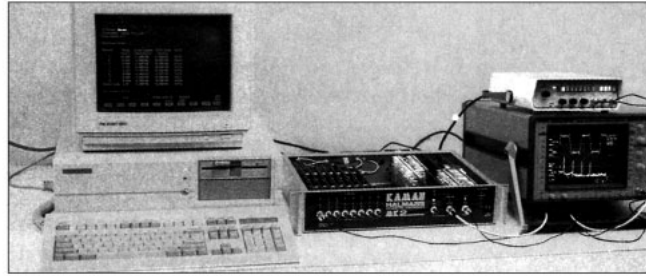


Figure 7. Mark 2 HALMARS Holometric Synthesizer and PC used to prepare and down-load programs.

cision is required in this regard and the PLL/PA circuit played a major role in achieving it. The PLL/PA improves performance in the “frequency multiplication” task normally relegated to a phase-locked loop in the generation of the required sines and cosines.

### Acknowledgements

William G. Flannelly developed the holometric philosophy and its application mathematics. Lee Pelham coordinated case programming and flight data acquisition. Randolph Perry led the digital design effort and John Ryan developed the firmware.

### Conclusions

Holometric Synthesis has been demonstrated as a feasible method for continuously monitoring the physical events in a helicopter’s rotor system. This same technology is potentially applicable to a broad range of rotating equipment. While initial calibration requires the use of a conventional slip-ring or rotating telemetry system, subsequent monitoring can be conducted without these elements. This results in a robust and inexpensive means of observation. S V